Aust. J. Plant Physiol., 1992, **19**, 519–38

Coupled Photosynthesis–Stomatal Conductance Model for Leaves of C_4 Plants*

G. James Collatz[A], *Miquel Ribas-Carbo*[B] *and Joseph A. Berry*[A]

[A] Carnegie Institution of Washington, Department of Plant Biology, 290 Panama Street, Stanford, CA 94305, USA.
[B] Department de Biologia Vegetal, Facultat de Biologia, Universitat de Barcelona, Avgda Diagonal, 645, 08028 Barcelona, Spain.

Abstract

Leaf based models of net photosynthesis (A_n) and stomatal conductance (g) are often components of whole plant, canopy and regional models of net primary productivity and surface energy balance. Since C_4 metabolism shows unique responses to environmental conditions and C_4 species are important agriculturally and ecologically, a realistic and accurate leaf model specific to C_4 plants is needed. In this paper we develop a simple model for predicting A_n and g from leaves of C_4 plants that is easily parameterised and that predicts many of the important environmental responses.

We derive the leaf model from a simple biochemical–intercellular transport model of C_4 photosynthesis that includes inorganic carbon fixation by PEP carboxylase, light dependent generation of PEP and RuBP, rubisco reaction kinetics, and the diffusion of inorganic carbon and O_2 between the bundle sheath and mesophyll. We argue that under most conditions these processes can be described simply as three potentially limiting steps. The leaf photosynthesis model treats A_n as first order with respect to either light, CO_2 or the amount of rubisco present and produces a continuous transition between limitations. The independent variables of the leaf photosynthesis model are leaf temperature (T_l), intercellular CO_2 levels and the absorbed quantum flux.

A simple linear model of g in terms of A_n and leaf surface CO_2 level (p_s) and relative humidity (h_s) is combined with the photosynthesis model to give leaf photosynthesis as a function of absorbed quantum flux, T_l and p_s and h_s levels.

Gas exchange measurements from corn leaves exposed to varied light, CO_2 and temperature levels are used to parameterise and test the models. Model parameters are determined by fitting the models to a set of 21 measurements. The behaviour of the models is compared with an independent set of 71 measurements, and the predictions are shown to be highly correlated with the data.

Under most conditions the leaf model can be parameterised simply by determining the level of rubisco in the leaves. The effects of light environment, nutritional status and water stress levels on A_n and g can be accounted for by appropriate adjustment of the capacity for rubisco to fix CO_2. We estimate rubsico capacity from CO_2 and light saturated photosynthesis although leaf nitrogen content or rubisco assays from leaf extracts could also be used for this purpose.

Introduction

Photosynthesis and stomatal movement are physiological processes that occur within leaves but whose influence on CO_2, water vapour and sensible heat fluxes extends to canopy, regional and global scales. Interest in predicting net primary productivity, hydrology and energy balance of vegetated surfaces in meteorological and climate models has lead to the use of simple leaf models for describing canopy processes (Lindroth and Halldin 1986; Sellers *et al.* 1986; Sellers 1987; Running and Coughlan 1988; Stewart 1988). Recently, more mechanistic models of photosynthesis and stomatal conductance at the leaf level have been proposed (Ball 1988; Leuning 1990; Tenhunen *et al.* 1990; Collatz *et al.* 1991; Sellers *et al.*

*This is CIW-DPB publ. No. 1139.

0310-7841/92/050519$10.00

1992) that derive from the C_3 photosynthesis model of Farquhar *et al.* (1980) and the empirical stomatal conductance model of Ball *et al.* (1987). These latter models are complete enough to include important responses yet simple enough to be easily parameterised and evaluated numerically.

Though the C_3 pathway of photosynthesis dominates most terrestrial ecosystems, another pathway, C_4, is important in certain agricultural and natural systems. The C_4 pathway is common among species native to tropical and subtropical grasslands, and important crop species such as corn, sorghum, sugar cane and pasture grasses possess C_4 photosynthesis. Accurate and simple models of photosynthesis and stomatal conductance of C_4 plants would be useful for predicting surface fluxes and energy balance in these systems.

C_4 differs from C_3 photosynthesis in several important biochemical and physiological properties. In both types, rubisco fixes CO_2 into the photosynthetic carbon reduction pathway common to all aerobic photosynthetic organisms, but the rubisco reaction is compartmented differently. In C_3 photosynthesis, CO_2 fixed by rubisco is obtained directly from the intercellular spaces of the leaf by diffusion, whereas in C_4 plants CO_2 is delivered to rubisco, which is localised in the bundle sheath chloroplasts, by a metabolic pump that concentrates CO_2. The elevated CO_2 concentrations maintained in the bundle sheath cells at the cost of additional ATP, has the benefit of inhibiting photorespiration. Consequently, C_4 plants lack several features of C_3 plants that are associated with photorespiration: (*a*) an O_2 dependent elevated CO_2 compensation point; (*b*) an inhibition of photosynthesis by O_2; and (*c*) a dependence of the quantum yield for photosynthesis on O_2, CO_2 and temperature. The kinetics of the photosynthetic CO_2 response also differ, because for C_4 metabolism the initial CO_2 fixation is via a more efficient catalyst, PEP carboxylase. These differences in function and compartmentation result in differing sensitivities of net photosynthesis to environmental conditions such as temperature, CO_2 and O_2 concentrations, light intensity and nitrogen availability. Generally these differences tend to favour C_4 plants over C_3 plants at high temperatures where photorespiration is stimulated. In addition C_4 plants may be favoured when nitrogen is limiting (Brown 1978). Finally, C_4 and C_3 plants exhibit differences in stomatal conductance under most conditions. C_4 plants in general have lower stomatal conductances than C_3 plants. Lower conductances coupled with higher photosynthetic capacity in leaves of C_4 plants result in higher water use efficiencies in comparison to leaves of C_3 plants (Pearcy and Ehleringer 1984).

These differences in physiological responses together with the ecological and agricultural importance of C_4 plants emphasise the need for a specific model describing C_4 photosynthesis and stomatal conductance. Grant (1989) developed a leaf model for C_3 and C_4 photosynthesis which he coupled with a radiation penetration model to predict canopy photosynthesis. His models are based on kinetic expressions for C_3 photosynthesis described in the models of Laing *et al.* (1974) and Farquhar *et al.* (1980). He modifies his C_3 model to make it behave like C_4 photosynthesis by arbitrarily increasing the chloroplastic CO_2 concentration 200-fold, thus simulating the CO_2 concentrating mechanism. These models, however, give unrealistic responses because of the way that the C_3 model is structured (see Collatz *et al.* 1990). In addition, his model does not accurately describe the kinetics of the CO_2 limited rate of C_4 photosynthesis.

We present here a C_4 photosynthesis–stomatal conductance model that is based on an updated version of the simple intercellular transport (ICT) model of C_4 photosynthesis developed by Berry and Farquhar (1978) and is linked with the stomatal model proposed by Ball *et al.* (1987). It is similar in form to the C_3 model of Collatz *et al.* (1991). The model predicts photosynthesis and stomatal conductance as a function of leaf temperature (T_l), photosynthetically active quantum flux density (Q_p), and CO_2 partial pressure and relative humidity at the leaf surface (p_s and h_s, respectively). The important adjustable parameters are the capacities of rubisco and PEP carboxylase to fix CO_2, which can be estimated from leaf photosynthetic responses to light and CO_2. We parameterise our model with a subset of leaf gas exchange data and then show a test of the model's capacity to predict

independent measurements of photosynthetic rate and stomatal conductance under a variety of conditions. The leaf model can be included within the framework of canopy and regional models to predict gross photosynthesis and transpiration from C_4 systems.

Theory

Stomatal Model

Stomatal conductance is sensitive to a number of environmental conditions such as light, humidity and CO_2 concentration. Efforts to predict stomatal conductance have focused on empirical analysis of stomatal response to variations in single factors taken one at a time and then the single factor responses are combined to give stomatal responses under conditions where all factors considered vary at the same time. The most commonly used model of this type is that of Jarvis (1976). Ball *et al.* (1987) proposed a model for stomatal conductance that derives primarily from two observations. First, that the ratio of the CO_2 concentration in the intercellular spaces and the leaf surface tends to be constant for leaves of the same photosynthetic pathway (i.e. C_3 or C_4) provided that atmospheric humidity remains constant (Wong *et al.* 1979; Ball and Berry 1982; Ramos and Hall 1982). Second, the data of Ball and others (Jarvis 1980; Leuning 1990; Mott and Parkhurst 1991) show that the sensitivity of stomata to a given vapour pressure deficit decreases as leaf temperature increases. Ball *et al.* (1987) formulated a simple linear model for stomatal conductance to water vapour consistent with these observations that takes the form

$$g = m\frac{A_n h_s P}{p_s} + b\,, \tag{1}$$

where h_s is the leaf surface relative humidity, P is the atmospheric pressure, p_s is the leaf surface CO_2 partial pressure, and m and b are the slope and intercept of a linear regression (see below). Ball (1988), Collatz *et al.* (1991), Leuning (1990) and Norman and Polley (1989) found that Eqn 1 accounts for much of the variation in stomatal responses observed in C_3 and C_4 leaves with different photosynthetic capacities and exposed to different temperature, light, humidity and CO_2 regimes.

Photosynthesis Model

Several models of C_4 photosynthesis at the cellular level have been proposed, all of which in essence link C_3 photosynthesis in the bundle sheath chloroplasts with a carbon pump

Table 1. Parameters used in the intercellular transport (ICT) model

Name	Symbol	Equation	Value	Source
Michaelis constant, CO_2	K_c	2A	140 Pa	Furbank *et al.* (1989)
O_2 inhibition constant	K_o	2A	34 kPa	Woodrow and Berry (1988)
CO_2/O_2-specificity ratio	τ	2A	2600	Collatz *et al.* (1991)
RuBP quantum requirement	α_r	3A	0·11 mol mol^{-1}	Berry and Farquhar (1978)
PEP quantum requirement	α_p	5A	0·167 mol mol^{-1}	Berry and Farquhar (1978)
Intercellular resistance to CO_2 diffusion	r_c	6A	500 m s mol^{-1}	Furbank *et al.* (1989)
Diffusivity of O_2 relative to CO_2	D	7A	40	Farquhar (1983)
Fraction of PSII in bundle sheath	λ	7A	0·1	Berry and Farquhar (1978)
Fractional RuBP quantum requirement	f	3	0·6	Berry and Farquhar (1978)
PEPcase rate constant for CO_2	k_p	4	0·7 mol m^{-2} s^{-1}	Data, Figs 1 and 2
Maximum rubisco capacity	V_{max}	5	39 μmol m^{-2} s^{-1}	Data, Figs 1 and 2
Leaf quantum absorptance	a	3	0·8	Norman and Polley (1989)
Intercellular partial pressure of O_2	O_i	7A	21 kPa	

driven by the activity of PEP carboxylase in the mesophyll leaf cells (Berry and Farquhar 1978; Peisker 1979; Farquhar 1983; Furbank and Hatch 1987). Carbon derived from intercellular CO_2 is fixed into C_4 acids in the mesophyll, transported to the bundle sheath cells and released as CO_2. Leakage of inorganic carbon from the bundle sheath cells to the intercellular spaces occurs because there is a large gradient in CO_2 concentration created by the pump. Following Berry and Farquhar (1978) the steady state balance of these transport processes can be simply expressed as

$$A = W_p - L\,, \tag{2}$$

where photosynthesis (A) is equal to the rate of C_3 photosynthesis in the bundle sheath chloroplasts. W_p is the velocity of the PEP carboxylase reaction and L is the flux of CO_2 leakage from the bundles sheath to the intercellular spaces of the mesophyll. Both A and L are themselves affected by the steady-state CO_2 concentration in the bundle sheath. We have developed analytical solutions to this intercellular transport (ICT) model that are further described in Appendix A. A simulation of photosynthetic response to intercellular partial pressure of CO_2 (p_i) is shown as the dashed curve in Fig. 2. Parameters used in the simulation are given in Table 1 and discussed in Appendix A.

Although the ICT model gives reasonable simulations, it is complex and unwieldy for routine simulations of leaf responses to environmental conditions. Analysis of the model behaviour shows that under most conditions, the CO_2 concentrating mechanism appears to work efficiently. Assuming that it is present without formally simulating its operation makes it possible to simplify the ICT model without sacrificing important response characteristics. The resulting model has a structure similar to the C_3 model of Collatz *et al.* (1991). The logic used to develop the simplified C_4 model from the more detailed kinetic expressions for the ICT model is discussed below.

At rate limiting light intensities the efficiency of CO_2 fixation with respect to absorbed light (quantum yield) determines the rate of photosynthesis, and empirical measurements indicate that the quantum yield is constant for C_4 plants over a wide range of conditions (Ehleringer and Björkman 1977; Ehleringer and Pearcy 1983). In terms of the ICT model the light dependent rate (J_i) as given in Eqn 3A (see Appendix *A*), reduces to

$$J_i = a\alpha_r f Q_p\,, \tag{3}$$

under conditions where the partial pressure of CO_2 in the bundle sheath (p_{bs}) is sufficiently high to suppress photorespiration. Other terms are: a, leaf absorptance, α_r, the intrinsic quantum yield of C_3 photosynthesis, f, the fraction of absorbed photons used by the C_3 reactions, and Q_p, the incident quantum flux density. In the simplified model the terms $\alpha_r f$ can be combined into a single constant. The theoretical value for this constant is 0·067 mol/mol which approximates the response of the ICT model at $Q_p \approx 50$ μmol m^{-2} s^{-1}.

At low CO_2 concentrations, empirical studies show that A increases linearly from the compensation point (near zero Pa) to rate saturation which occurs at an intercellular CO_2 partial pressure (p_i) of about 10 Pa. The slope is largely independent of O_2. In terms of the ICT model the absence of a strong O_2 dependence arises because the rate is controlled by the initial CO_2 fixation reaction (W_p, Eqn 4A) less the leak rate (L, Eqn 6A) both of which are independent of O_2 partial pressure. The CO_2 limited flux (J_c) may be expressed as

$$J_c = p_i\left(k_p - \frac{L}{p_i}\right)/P\,, \tag{4}$$

where k_p is a pseudo-first-order rate constant for PEP carboxylase with respect to p_i. The ICT model predicts that L/p_i is small when p_i is low and increases non-linearly as A approaches the limit imposed by the V_{max} of rubisco (J_e, see below).

In terms of the simplifed model, $(k_p - L/p_i)$ is taken as a constant, k, which may be empirically evaluated from leaf gas exchange measurements at rate limiting p_i levels. The deviation of dA/dp_i from k as p_i increases is empirically taken into account through the curvature or co-limitation parameter, β (Eqn 3B, Table 2). The models presented here do not explicitly treat the fact that PEP carboxylase uses HCO_3^- rather than CO_2 as substrate or the observations that this enzyme's activity is regulated by activation processes and metabolic pool sizes (Hatch 1987; Leegood and von Caemmerer 1989).

Empirical observations show that, when J_i and J_c are not limiting, the rate of assimilation approaches a rate, J_e, that is largely independent of CO_2 and light. In the ICT model the rate under these conditions is controlled by the capacity for CO_2 fixation by rubisco (Eqn 2A). The high CO_2 concentration in the bundle sheath chloroplasts is close to saturating for rubisco, and the rate under these conditions approaches

$$J_e = V_{max}. \tag{5}$$

Other reactions downstream from rubisco could become limiting under some circumstances (as occurs in C_3 photosynthesis: see Collatz *et al.* 1991) but we currently lack an experimental basis for distinguishing this type of limitation for one imposed by V_{max} alone. The ICT model predicts fairly smooth transitions between the CO_2 limited and V_{max} limited states with relatively little co-limitation (Fig. 2). The ICT model described here does not include effects of temperature but these can be added by including the temperature dependences of the kinetic parameters in the model.

Thus, we can simplify the ICT model to describe just these three limiting states. The relationships between limiting steps and the rate of net photosynthesis (A_n) for the simplified model can be expressed as

$$A_n \approx \min \left\{ \begin{array}{l} J_i, f(\alpha, Q_p) \\ J_c, g(p_i, k, T_l) \\ J_e, h(V_{max}, T_l) \end{array} \right\} - R_d, i(T_l), \tag{6}$$

where f–i denote separate functions of, T_l is leaf temperature, α is the product of leaf absorptance and the intrinsic quantum utilisation efficiency and R_d is the rate of CO_2 release or respiration. Equation 6 is the same general form proposed by Farquhar *et al.* (1980) for a model of C_3 photosynthesis and used by others (Kirschbaum and Farquhar 1984; Collatz *et al.* 1991). Following Collatz *et al.* (1991) we used nested quadratic formulations (Eqns 2B and 3B, Appendix B) to pick the subprocess most limiting and to assign a gradual transition from one limitation to another with some specific curvature (see Collatz *et al.* 1990).

Table 2. Parameters used in the simplified C_4 photosynthesis model

Name	Symbol	Equation	Value (Q_{10})
Initial slope of photosynthetic CO_2 response	k	6	0·7 mol m^{-2} s^{-1} (2)
Maximum rubisco capacity	V_{max}	6	39 μmol m^{-2} s^{-1} (2)
Initial slope of photosynthetic light response	α	6	0·04 mol m^{-1}
Leaf respiration	R_d	6	0·8 μmol m^{-2} s^{-1} (2)
Stomatal slope factor	m	1	3·0
Stomatal intercept factor	b	1	0·08
Atmospheric pressure	P	1	10^5 Pa
Curvature parameter	θ	2B	0·83
Curvature parameter	β	3B	0·93

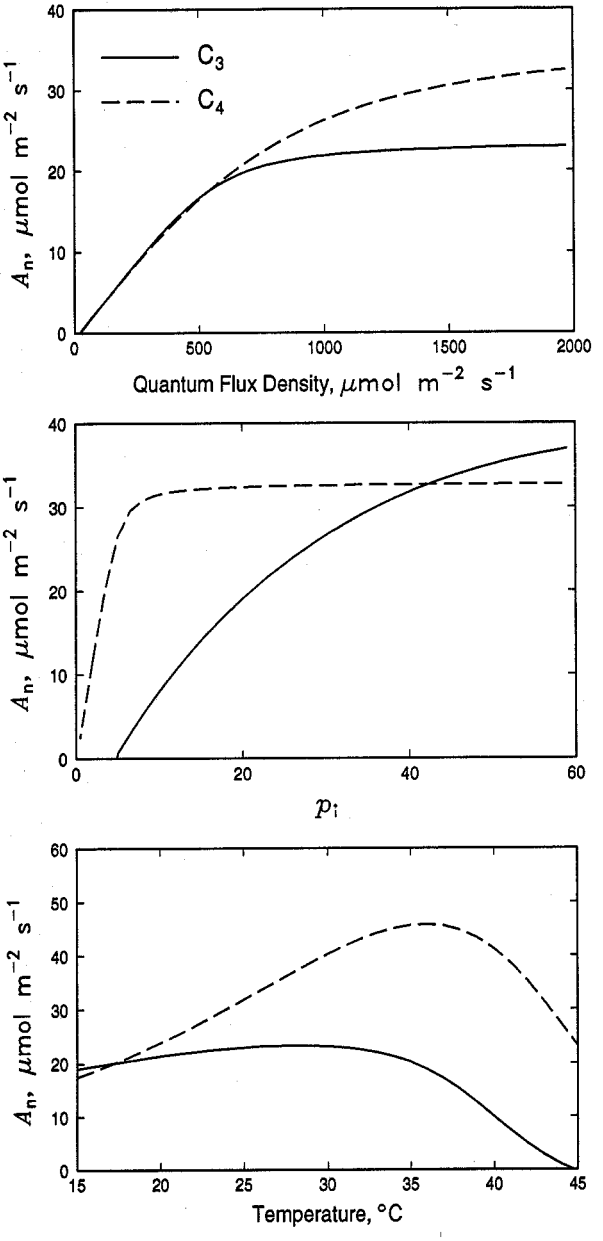

Fig. 1. Comparison of the simulated responses of C_3 (solid line) and C_4 (dashed line) photosynthesis. Response of net photosynthesis (*a*) to quantum flux, at 25°C, and intercellular CO_2 partial pressure (p_i) of 25 and 15 Pa for C_3 and C_4 respectively; (*b*) to intercellular CO_2 partial pressure at 25°C and quantum flux of 1500 μmol m^{-2} s^{-1} and (*c*) to leaf temperature at p_i of 25 and 15 Pa for C_3 and C_4 respectively and quantum flux of 1500 μmol m^{-2} s^{-1}. Parameters used in the simulations of C_3 photosynthesis are given by Collatz *et al.* (1991) except that the substrate saturated rubisco capacity is set to 90 μmol m^{-2} s^{-1}.

The simplifed model has the advantages of having an analytical solution and a reduced number of parameters (5 *v.* 13).

The general response characteristics of the simplifed C_4 model are shown in Fig. 1 together with those of a C_3 model of Collatz *et al.* (1991) for comparison. The parameters of the C_4 model are given in Table 2 and their estimation is described in detail later. To summarise briefly, Fig. 1*a* shows the greater photosynthetic capacity and slower approach to light saturation that are characteristic of C_4 photosynthesis (Osmond *et al.* 1980). At 25°C the slope of the light response curve at low quantum fluxes (the quantum yield) is similar for the two types. However, the quantum yield of C_3 photosynthesis is dependent on temperature, O_2 and CO_2 partial pressures (not shown) which is not the case for C_4 plants. This results in higher quantum yields for C_3 plants at lower temperatures while the reverse is true at higher temperatures (Ehleringer and Björkman 1977).

Figure 1*b* illustrates responses of A_n to the partial pressure of CO_2 in the intercellular spaces (p_i). The greater initial slope and the rapid saturation with respect to p_i is typical of C_4 photosynthesis (Osmond *et al.* 1980). At p_i levels usually observed in non-stressed C_4 leaves (>10 Pa) A_n approaches the V_{max} capacity for rubisco. C_3 leaves, on the other hand, may reach similar values of A_n at p_i levels twice normal, but A_n remains a fraction of V_{max} (90 μmol m^{-2} s^{-1}) for rubisco. The absence of significant rates of photorespiration in C_4 plants allows A_n to remain positive at low p_i (<1 Pa) whereas C_3 photosynthesis is characterised by negative rates below the CO_2 compensation point (*c.* 4 Pa).

Figure 1*c* shows the differences between C_3 and C_4 pathways in response to temperature at high quantum flux and constant p_i. The low photorespiration rates and ability to photosynthesise at close to the full rubisco capacity results in higher A_n at high temperatures in C_4 plants. These differences disappear or are reversed at lower temperatures. The high and low temperature inhibition functions are given in Appendix B. The parameters in these functions can be adjusted to give different temperature response patterns (see below).

Leaves of C_4 plants may show variable photosynthetic responses depending upon the light intensity for growth (Louwerse and Zweerde 1977; Robichaux and Pearcy 1980; Wong *et al.* 1985*a*), nitrogen nutrition (Wong 1979; Wong *et al.* 1985*a*; Sage and Pearcy 1987) or drought stress (Ehleringer 1983; Wong *et al.* 1985*b*). These variations can generally be accommodated by adjusting the parameters V_{max}, k and R_d of our model as described below in the experimental methods. Accounting for adaptation and acclimation of C_4 photosynthesis to growth temperature regimes (Björkman and Pearcy 1971; Pearcy 1977) may also require adjusting the high and low temperature stability parameters of the model (see Appendix B).

Coupling Photosynthesis to Stomatal Conductance

p_i appears as an independent variable in the photosynthesis model (Eqns 6 and 3B) but it is a state variable at the leaf level determined by the uptake of CO_2 by photosynthesis and the supply of CO_2 by diffusion through the stomatal pores. Knowing A_n (Eqn 3B) and g (Eqn 1), we can obtain p_i from the one-dimensional model for diffusion of CO_2,

$$p_i = p_s - A_n 1{\cdot}6P/g\,, \tag{7}$$

where the proportionality factor 1·6 accounts for the ratio of the diffusivities of CO_2 and H_2O vapour in the stomatal pore (Cowan and Troughton 1971) and P is atmospheric pressure.

Equation 7 together with Eqns 1 and 6 can be solved simultaneously to give g and A_n in terms of Q_p, T_l, h_s and p_s. The exact solution is a cubic equation described in Appendix C. A numerical approach similar to that of Collatz *et al.* (1991) can be used to couple this model with leaf energy balance and boundary layer diffusion.

Materials and Methods

The fluxes of CO_2 and H_2O vapour were measured with an open gas exchange system similar to that described and illustrated in fig. 11.4 of Field *et al.* (1989). Portions of corn leaves were enclosed in a water jacketed chamber in which gas fluxes from the top and bottom of leaves were measured separately. Boundary layer conductance was estimated at 1·2 μmol m^{-2} s^{-1} for each side based on measured temperature, area and evaporation rates from moist filter paper. Variables derived from the flux measurements (A_n, g, p_s, h_s and p_i) were calculated according to von Caemmerer and Farquhar (1981) and Ball (1987) for each leaf surface. A_n and g are reported as the sums of measurements from both sides of the leaves. h_s, p_s and p_i were estimated from the flux-weighted averages of estimates from each side. Corn plants were well fertilised and grown in pots ($\approx$4 L) in a glasshouse at Stanford during the summer. A set of measurements in which quantum flux and the partial pressure of CO_2 in the intercellular spaces were varied while h_s and T_l remained relatively constant ($h_s = 0{\cdot}7$–$0{\cdot}8$, $T_l = 25 \pm 1$°C, $n = 21$) were used to set the adjustable parameters of the model.

Equation 6 was solved by selecting the smaller roots of nested quadratic equations (Eqns 2B and 3B). The adjustable parameters V_{max}, k, α, θ, and β were estimated by non-linear regression using a subset of gas exchange measurements. R_d was estimated by measuring CO_2 flux from darkened leaves. Q_{10} values for V_{max}, k and R_d were specified as given in Table 2. The parameters m and b of the stomatal model (Eqn 1) were determined by linear regression using measured values of A_n, h_s and p_s.

An independent set of measurements ($n = 71$) over a broad range of CO_2 partial pressure, quantum flux, temperature and humidity (photon flux density, dark to 1960 μmol m^{-2} s^{-1}; CO_2 partial pressure, 3–34 Pa; leaf tempeature, 18·5–32·5°C, surface relative humidity, 43–84%) were used to test the accuracy of the parameterised models.

Results

The predictions of A_n and g using fitted parameters were highly correlated ($r^2 = 0{\cdot}99$ and 0·93 respectively) with the data used to parameterise the models. Fig. 2 shows the

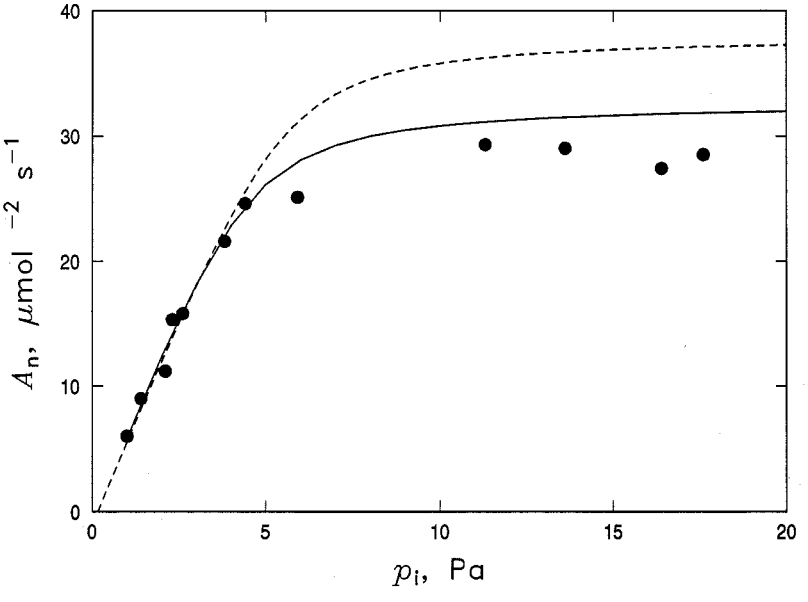

Fig. 2. Measured and predicted responses of photosynthesis (A) to the CO_2 partial pressure in the intercellular spaces of the leaf. Symbols refer to measurements. The solid line is the predicted response based on the leaf photosynthesis model using parameter values giving the best fit to measurements shown here and in Fig. 3. The dashed line shows the response predicted by the intercellular transport model described in Appendix A. Leaf temperature is 25°C and incident quantum flux is 1400 μmol m^{-2} s^{-1}.

response of A_n to p_i obtained from measurements (symbols) and the model (solid line). We measured CO_2 efflux in the dark at 25°C to be 0·8 μmol m^{-2} s^{-1} and this value is added to the measured A_n to give A. As is generally observed in C_4 plants A saturates abruptly as p_i reaches CO_2 partial pressures over 10 Pa. This is reflected in the value of

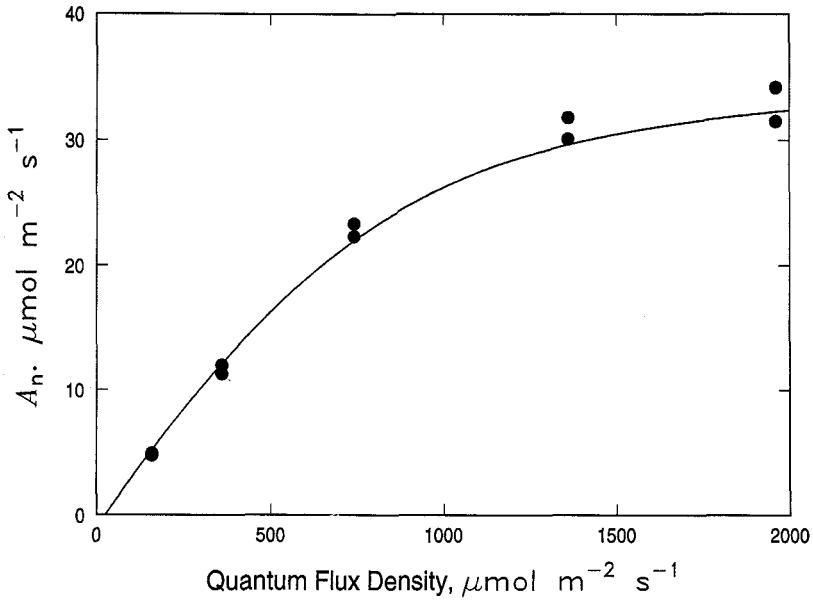

Fig. 3. Response of photosynthesis to incident quantum flux density. Symbols represent measurements and solid line gives response of the model using fitted parameters. Leaf temperature is 25°C and intercellular CO_2 partial pressure is 15 Pa.

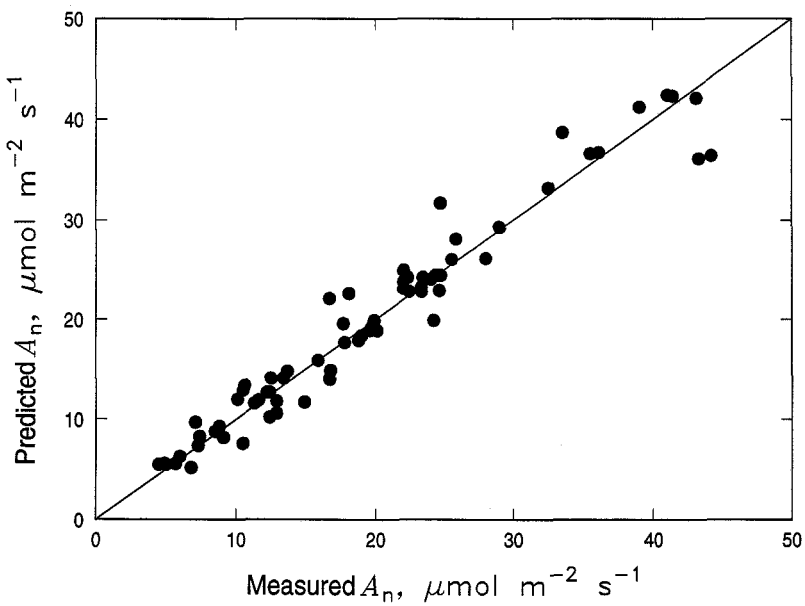

Fig. 4. Photosynthesis predicted by the simplified C_4 model plotted against measured rates. The line represents the 1 to 1 relationship between predicted and measured rates.

the fitted curvature parameter, β, which is close to 1 ($\beta = 0{\cdot}93$). On the other hand, A saturates more gradually with respect to quantum flux as shown in Fig. 3 (curvature parameter $\theta = 0{\cdot}83$) causing A to continue increasing beyond full sun quantum fluxes.

Figure 4 shows a comparison of measured A_n to A_n predicted by the model using a set of data ($n = 71$) independent of that used to parameterise the photosynthesis model (see Figs 2 and 3; Table 2). Linear regression of the data for a line passing through the origin shows predictions are highly correlated with measurements ($r^2 = 0{\cdot}989$), and the slope of the regression line is not significantly different from 1 ($P > 0{\cdot}999$).

A plot of measured g versus the product ($h_s \times A_n \times P/p_s$) is shown in Fig. 5 using the same data set used to parameterise the photosynthesis model (Figs 2 and 3). The value for the slope factor, m, of 3·06 (Table 2) is similar to that reported by Norman and Polley (1989) and Ball (1988) for a number of C_4 species, and is less than half of the values reported for C_3 species (Ball 1988; Leuning 1990). The value for the intercept, b, of 0·08 is somewhat higher than that found by Norman and Polley (1988) and Ball (1988).

In Fig. 6, the 71 independent measurements of g are plotted against ($h_s \times A_n \times P/p_s$) as open symbols and the regression line for this data is dashed. For comparison the parameterisation data and regression line from Fig. 4 are re-plotted here as solid symbols and line respectively. The slope factor m for the validation data set is 3·13 and the intercept b is 0·08 ($r^2 = 0{\cdot}91$). The similar parameter values obtained for the parameterisation and validation data sets and high correlation coefficient show that the stomatal model can be accurately parameterised from a relatively small number of measurements. Fitting the data to a second degree polynomial resulted in a small increase in the correlation coefficient ($r^2 = 0{\cdot}92$).

A test of the stomatal conductance and photosynthesis models in combination is provided by using predicted A_n rather than the measured A_n in the stomatal model (Eqn 1). A plot of g predicted from the photosynthesis model and the fitted parameters m and b in relation to measured g is shown in Fig. 7. The regression line is constrained to pass through the

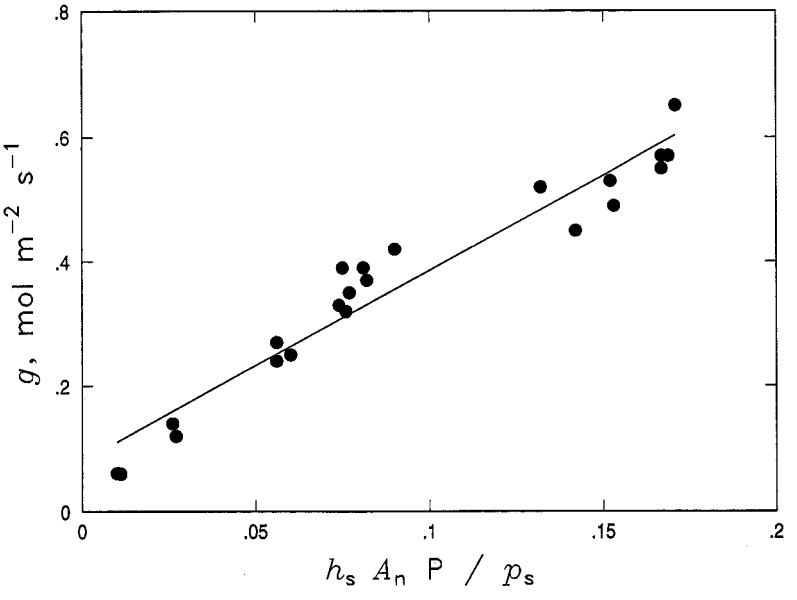

Fig. 5. Stomatal conductance as a function of the product of surface humidity, net photosynthesis and the recriprocal of surface CO_2 partial pressure. The regression line is given as $y = 3{\cdot}06x + 0{\cdot}08$ ($r^2 = 0{\cdot}93$).

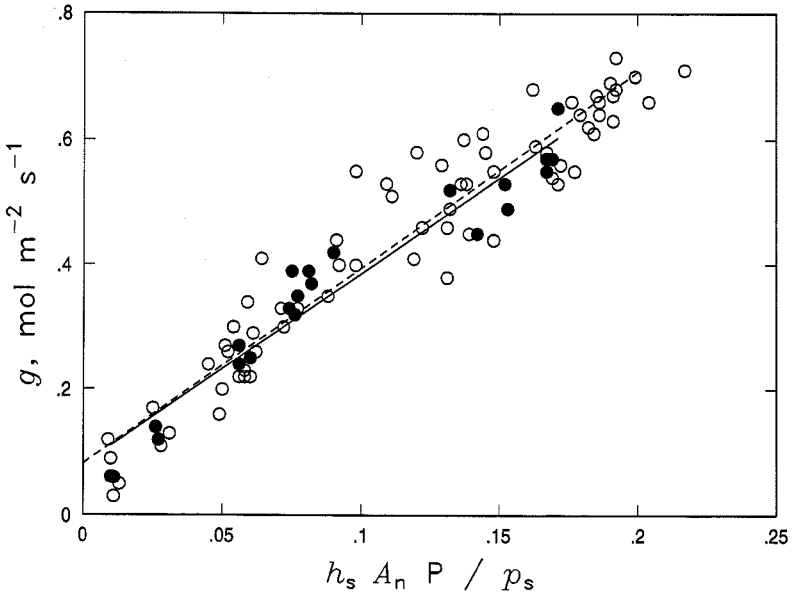

Fig. 6. Predicted stomatal conductance as a function of net photosynthesis, surface relative humidity and CO_2 partial pressure from an independent data set (open circles). Data and regression line from Fig. 4 (closed symbols and solid line respectively) are included for comparison. The independent data set yields the linear regression equation $y = 3{\cdot}13x + 0{\cdot}08$ ($r^2 = 0{\cdot}91$).

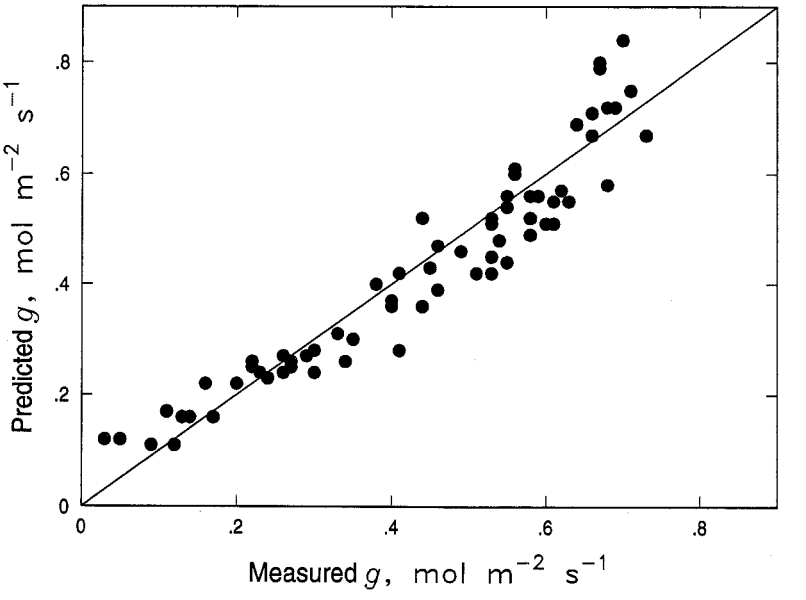

Fig. 7. Stomatal conductance predicted from measured net photosynthesis in comparison to measured stomatal conductance. The line represents the 1 to 1 relationship between predicted and measured rates.

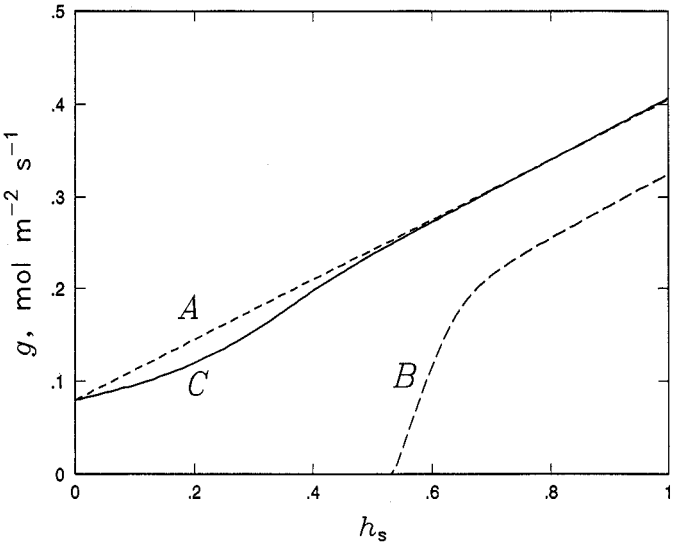

Fig. 8. Simulated response of stomatal conductance to leaf surface relative humidity using the coupled photosynthesis–stomatal conductance model. Curve *A* is the response in the absence of photosynthesis feedback on *g*. Curve *B* includes feedback interaction between net photosynthesis and stomatal conductance when the intercept *b* of the stomatal model is set to zero. Curve *C* is the same as *B* except the parameter *b* is set to 0·08 (Table 2). For these simulations quantum flux is 1500 μmol m^{-2} s^{-1}, leaf temperature is 25°C and surface CO_2 partial pressure is 30 Pa.

origin. The correlation between measured and predicted *g* remains high for the linear regression ($r^2 = 0{\cdot}984$) and the slope of the regression line is not significantly different from 1 ($P > 0{\cdot}999$).

We did not determine whether our measurements of *g* reflected a spatially homogeneous distribution of conductance across the measured leaf surfaces. It is possible that our calculations of average p_i levels could be in error due to patchy stomatal closure (Laisk 1983; Daley *et al.* 1989; Farquhar 1989). However, because of the linear responses of A_n to p_i at both high and low CO_2 partial pressures (Figs 1*b* and 2), patchy stomatal closure should be a problem only when photosynthesis of some parts of the leaf is saturated with respect to CO_2 while in others parts photosynthesis is CO_2 limited. Under these conditions the calculated p_i and thus A_n would be overestimated. The effects of non-homogeneous distribution of *g* are not large enough to cause serious discrepancies between predictions of our model and our leaf measurements.

Discussion

The ICT model discussed here includes consideration of photorespiration and CO_2 and O_2 leakage as component processes of C_4 photosynthesis. Analysis of the behaviour of the ICT model shows that photorespiration is negligible under most conditions if the CO_2 concentrating mechanism is given plausible parameters. The simplified model does not explicitly treat photorespiration or the CO_2 concentrating mechanism but these processes are implicitly contained in the structure of the model. The advantages gained from this simplification are a more tractable model that can be solved analytically and a relatively small number of adjustable parameters. These characteristics make this model useful as a subcomponent of more complex models designed to predict photosynthesis at larger scales such as the leaf and canopy.

Of the five main parameters in the simplified photosynthesis model (Eqn 6), V_{max} and k are likely to be the most variable among leaves grown under different conditions. Additionally, R_d may vary in a systematic way with growth conditions. Several studies (Wong *et al.* 1979; Robichaux and Pearcy 1980; Wong *et al.* 1985*a*) show that A_n measured at high light both under the CO_2 saturation (V_{max} limited) and CO_2 limitation (k limited) varies with the nitrogen nutrition and light levels that C_4 plants are exposed to during growth. Robichaux and Pearcy (1980) and Pearcy (1977) showed that R_d co-varies with CO_2-saturated A_n for differing growth conditions. For unstressed leaves of corn we obtained $V_{max} = 39$ μmol m^{-2} s^{-1}, $k = 0{\cdot}7$ mol m^{-2} s^{-1} and $R_d = 0{\cdot}8$ μmol m^{-2} s^{-1}, or $k = 18 \times 10^3 V_{max}$ and $R_d = 0{\cdot}021 V_{max}$. Assuming V_{max}, R_d and k co-vary with leaf nitrogen and remain approximately proportional to one another as conditions change, V_{max} (or its surrogate, leaf nitrogen) becomes the most important parameter to estimate in our C_4 model. This is also the case for the C_3 model of Collatz *et al.* (1991). V_{max} can be estimated from leaf photosynthesis measurements as was done here or possibly from leaf nitrogen levels.

We expect that the other parameters of the simplified model will vary over smaller ranges of values than V_{max} and k. For example, the kinetic parameters of rubisco, PEP carboxylase and respiration are biochemical properties that should not vary much from leaf to leaf. Similarly, the Q_{10} values for the temperature responses of V_{max}, k and R_d under non-stressed conditions should not vary with the photosynthetic capacity of the leaf. Studies of rubisco (Badger and Collatz 1977), R_d (Pearcy 1977; Polley *et al.* 1992) and k (Polley *et al.* 1992 and our measurements) were used to select the Q_{10} values used here. Furthermore, α may also be conservative since leaf absorptance and the intrinsic quantum yield of C_4 photosynthesis vary over narrow ranges and are fairly independent of environmental conditions. Finally, the fitted values for the parameters θ and β which reflect the degree of curvature in the light and CO_2 responses of A, are also likely to be similar for most C_4 plants.

The stomatal model contains two parameters, the slope m and intercept b of Eqn 1. The fitted values for these parameters are similar to those reported by others for C_4 plants (Ball 1988; Norman and Polley 1989) and may not need to be routinely adjusted. The smaller value for m found in C_4 plants relative to C_3 plants is consistent with the observation that g is usually smaller in the former for a given set of conditions.

The intercept, b, of the linear equation Eqn 1 gives a minimum value for g as $h_s A_n P / p_s \rightarrow 0$. The existence of a positive intercept in this equation has important implications for the behaviour of the coupled photosynthesis–stomatal conductance model. This is shown graphically in Fig. 8 which gives simulations of g as a function of h_s. Setting b to zero causes g to go to zero at moderate humidities, because humidity-induced stomatal closure causes A_n to decrease as p_i is reduced, which in turn closes stomata further (a positive feedback loop). This behaviour can be illustrated algebraically by combining Eqns 1 and 7 and setting $b = 0$ to give

$$p_i = p_s(1 - 1{\cdot}6/mh_s) . \tag{8}$$

It is clear from Eqn 8 that as h_s approaches $1{\cdot}6/m$ or $0{\cdot}53$, p_i approaches zero, as must A and g. If we use the fitted value of b (curve C in Fig. 8), the modelled response of g to h_s is more realistic. The minimum value of g that we measured in the dark, however, is much smaller than the fitted value of b at high light levels ($0{\cdot}01$ *v.* $0{\cdot}08$) implying that minimum conductance is dependent to some extent on light. If b is held constant, transpiration could be overestimated at night, especially from canopies with high leaf area index. One possible approach to this problem is to make b dependent upon Q_p. For instance, a day–night switch or a light-dependent exponential function similar to that used to describe temperature inhibition (Eqn 5B) can be used to obtain a low minimum value of g at night while avoiding the unrealistic behaviour at low h_s (Fig. 8) and high Q_p. It seems possible that other conditions such as severe drought stress may affect the minimum value of g as well, though we currently have no evidence to support this. Further studies on the response

of g to stress and low light conditions are needed in order to resolve the behaviour of the minimum g and to improve the model's treatment of this phenomenon.

The combination of Eqns 1, 6 and 7 takes into account important environmental and physiological factors that affect photosynthesis and stomatal conductance in leaves of C_4 plants with minimum complexity. Such a model should be useful for predicting C_4 canopy photosynthesis provided leaf surface conditions can be specified. Simple canopy models which assume single bulk values for surface concentrations through the whole canopy may be adequate for predicting fluxes of CO_2 and H_2O (Goudriaan 1989; Sellers *et al.* 1992) from canopies, when used in conjunction with a radiation penetration model and the leaf photosynthesis model reported here.

Simple yet realistic models of photosynthesis and stomatal conductance of canopies of C_4 plants should be useful for the study of the impacts of large-scale land use change in the tropics. Since rainforests which are largely composed of C_3 species are increasingly being replaced by tropical pasture grasses which are C_4 type, characteristics of C_4 metabolism such as high temperature tolerance (see Fig. 1*c*) and lower stomatal conductance could alter regional hydrology and surface energy balance (Shukla *et al.* 1990). A realistic model of leaf gas exchange in C_4 plants such as that reported here can be incorporated as an interactive part of an atmospheric climate model to predict the effects of land use change in the tropics.

Acknowledgment

This work was supported in part by an EOS-IDS grant from NASA.

References

Badger, M. R., and Collatz, G. J. (1977). Studies on the kinetic mechanism of ribulose-1,5-bisphosphate carboxylase and oxygenase reactions, with particular reference to the effect of temperature on the kinetic parameters. *Carnegie Institution of Washington Yearbook* **76**, 355–61.

Ball, J. T. (1987). Calculations related to gas exchange. In 'Stomatal Function'. (Eds E. Zeiger, G. D. Farquhar and I. R. Cowan.) pp. 446–76. (Stanford University Press: Stanford, California.)

Ball, J. T. (1988). An analysis of stomatal conductance. Ph.D. Thesis, Stanford University.

Ball, J. T., and Berry, J. A. (1982). The C_i/C_s ratio: A basis for predicting stomatal control of photosynthesis. *Carnegie Institution of Washington Yearbook* **81**, 88–92.

Ball, J. T., Woodrow, I. E., and Berry, J. A. (1987). A model predicting stomatal conductance and its contribution to the control of photosynthesis under different environmental conditions. In 'Progress in Photosynthesis Research'. (Ed. J. Biggins.) Vol. 4, pp. 221–4. (Nijhoff: Dordrecht.)

Berry, J. A., and Björkman, O. (1980). Photosynthetic temperature response and adaptation to temperature in higher plants. *Annual Review of Plant Physiology* **31**, 491–543.

Berry, J. A., and Farquhar, G. D. (1978). The CO_2 concentrating function of C_4 photosynthesis: a biochemical model. In 'Proceedings of the 4th International Congress on Photosynthesis'. (Eds D. Hall, J. Coombs and T. Goodwin.) pp. 119–31. (Biochemical Society: London.)

Björkman, O., and Pearcy, R. W. (1971). Effect of growth temperature on the fixation *in vitro* in C_3 and C_4 species. *Carnegie Institution of Washington Yearbook* **70**, 511–20.

Brown, R. H. (1978). A difference in N use efficiency in C_3 and C_4 plants and its implications in adaptation and evolution. *Crop Science* **18**, 93–8.

Caemmerer, S. von, and Farquhar, G. D. (1981). Some relationships between the biochemistry of photosynthesis and the gas exchange of leaves. *Planta* **153**, 376–87.

Collatz, G. J., Berry, J. A., Farquhar, G. D., and Pierce, J. (1990). The relationship between the rubisco reaction mechanism and models of photosynthesis. *Plant, Cell and Environment* **13**, 219–25.

Collatz, G. J., Ball, J. T., Grivet, C., and Berry, J. A. (1991). Physiological and environmental regulation of stomatal conductance, photosynthesis and transpiration: a model that includes a laminar boundary layer. *Agricultural and Forest Meteorology* **54**, 107–36.

Cowan, I. R., and Troughton, J. H. (1971). The relative role of stomata in transpiration and assimilation. *Planta* **97**, 325–36.

Daley, P. F., Raschke, K., Ball, J. T., and Berry, J. A. (1989). Topography of photosynthetic activity of leaves obtained from video images of chlorophyll fluorescence. *Plant Physiology* **90**, 1233–8.

Ehleringer, J. (1983). Ecophysiology of *Amaranthus palmeri*, a sonoran desert summer annual. *Oecologia* **57**, 107–12.

Ehleringer, J., and Björkman, O. (1977). Quantum yields for CO_2 uptake in C_3 and C_4 plants: dependence on temperature, CO_2 and O_2 concentration. *Plant Physiology* **59**, 86–90.

Ehleringer, J., and Pearcy, R. W. (1983). Variation in quantum yield for CO_2 uptake among C_3 and C_4 plants. *Plant Physiology* **73**, 555–9.

Farquhar, G. D. (1983). On the nature of carbon isotope discrimination in C_4 species. *Australian Journal of Plant Physiology* **10**, 205–26.

Farquhar, G. D. (1989). Models of integrated photosynthesis of cells and leaves. *Philosophical Transactions of the Royal Society of London* **B323**, 357–67.

Farquhar, G. D., Caemmerer, S. von, and Berry, J. A. (1980). A biochemical model of photosynthetic CO_2 assimilation in leaves of C_3 plants. *Planta* **149**, 78–90.

Field, C. B., Ball, J. T., and Berry, J. A. (1989). Photosynthesis: principles and field techniques. In 'Plant Physiological Ecology: Field Methods and Instrumentation'. (Eds R. W. Pearcy, J. Ehleringer, H. A. Mooney and P. W. Rundel.) pp. 209–53. (Chapman and Hall: London.)

Furbank, R. T., and Hatch, M. D. (1987). Mechanism of C_4 photosynthesis. The size and composition of the inorganic carbon pool in bundle sheath cells. *Plant Physiology* **85**, 958–64.

Furbank, R. T., Jenkins, C. L. D., and Hatch, M. D. (1989). CO_2 concentrating mechanism of C_4 photosynthesis. Permeability of isolated bundle sheath cells to inorganic carbon. *Plant Physiology* **91**, 1364–71.

Goudriaan, J. (1989). Simulation of micrometeorology of crops, some methods and their problems, and a few results. *Agricultural and Forest Meteorology* **47**, 239–58.

Grant, R. F. (1989). Test of a simple biochemical model for photosynthesis of maize and soybean leaves. *Agricultural and Forest Meteorology* **48**, 59–74.

Hatch, M. D. (1987). C_4 photosynthesis: a unique blend of modified biochemistry, anatomy and ultrastructure. *Biochimica et Biophysica Acta* **895**, 81–106.

Jarvis, P. G. (1976). The interpretations of the variation in leaf water potential and stomatal conductance found in canopies in the field. *Philosophical Transactions of the Royal Society of London* **B273**, 593–610.

Jarvis, P. G. (1980). Stomatal response to water stress in conifers. In 'Adaptation of Plants to Water and High Temperature Stress'. (Eds N. C. Turner and P. J. Kramer.) pp. 105–22. (Wiley: New York.)

Kirschbaum, M. F., and Farquhar, G. D. (1984). Temperature dependence of whole-leaf photosynthesis in *Eucalyptus pauciflora* Sieb. ex Spreng. *Australian Journal of Plant Physiology* **11**, 519–38.

Laing, W. A., Ogren, W. L., and Hageman, R. H. (1974). Regulation of soybean net photosynthetic CO_2 fixation by the interaction of CO_2, O_2 and ribulose-1,5-diphosphate carboxylase. *Plant Physiology* **54**, 678–85.

Laisk, A. (1983). Calculations of leaf photosynthetic parameters considering the statistical distribution of stomatal apertures. *Journal of Experimental Botany* **34**, 1627–35.

Leegood, R. C., and Caemmerer, S. von (1989). Some relationships between contents of photosynthetic intermediates and the rate of photosynthetic carbon assimilation in leaves of *Zea mays* L. *Planta* **178**, 258–66.

Leuning, R. (1990). Modelling stomatal behaviour and photosynthesis of *Eucalyptus grandis*. *Australian Journal of Plant Physiology* **17**, 159–75.

Louwerse, W., and Zweerde, W. V. D. (1977). Photosynthesis, transpiration and leaf morphology of *Phaseolus vulgaris* and *Zea mays* grown at different irradiances in artificial and sunlight. *Photosynthetica* **11**, 11–21.

Mott, K. A., and Parkhurst, D. F. (1991). Stomatal responses to humidity in air and helox. *Plant, Cell and Environment* **14**, 509–15.

Norman, J. M., and Polley, W. (1989). Canopy photosynthesis. In 'Photosynthesis'. (Ed. W. R. Briggs.) pp. 227–41. (Liss: New York.)

Osmond, C. B., Björkman, O., and Anderson, D. J. (1980). 'Physiological Processes in Plant Ecology: Toward a Synthesis with *Atriplex*.' Ecological Studies Vol. 36. (Eds W. D. Billings, F. Golley, O. L. Lange and J. S. Olson.) (Springer-Verlag: Berlin.)

Pearcy, R. W. (1977). Acclimation of photosynthetic and respiratory carbon dioxide exchange to growth temperature in *Atriplex lentiformes* (Torr.) Wats. *Plant Physiology* **59**, 795–9.

Pearcy, R. W., and Ehleringer, J. (1984). Comparative ecophysiology of C_3 and C_4 plants. *Plant, Cell and Environment* **7**, 1–13.

Peisker, M. (1979). Conditions for low, and oxygen-independent, CO_2 compensation concentrations in C_4 plants as derived from a simple model. *Photosynthetica* **13**, 198–207.

Polley, H. W., Norman, J. M., Arkebauer, T. J., Walter-Shea, E. A., Greegor, D. H. Jr, and Bramer, B. (1991). Leaf gas exchange of *Andropogon gerardii* Vitman, *Panicum virgatum* L. and *Sorghastrum nutans* (L.) Nash in a tallgrass prairie. *Journal of Geophysical Research* (in press).

Press, W. H., Flannery, B. P., Teukolsky, S. A., and Vetterling, W. T. (1989). 'Numerical Recipes. The Art of Scientific Computing (FORTRAN version).' (Cambridge University Press: Cambridge.)

Ramos, C., and Hall, A. E. (1982). Relationships between leaf conductance, intercellular CO_2 partial pressure and CO_2 uptake rate in two C_3 and C_4 plant species. *Photosynthetica* **16**, 343–55.

Robichaux, R. H., and Pearcy, R. W. (1980). Environmental characteristics, field water relations and photosynthetic responses of C_4 Hawaiian *Euphorbia* species from contrasting habitats. *Oecologia* **47**, 99–105.

Running, S. W., and Coughlan, J. C. (1988). A general model of forest ecosystem processes for regional applications. I. Hydrological balance, canopy gas exchange and primary production processes. *Ecological Modelling* **42**, 125–54.

Sage, R. F., and Pearcy, R. W. (1987). The nitrogen use efficiency of C_3 and C_4 plants. II. Leaf nitrogen effects on the gas exchange characteristics of *Chenopodium album* (L.) and *Amaranthus retroflexus* (L.). *Plant Physiology* **84**, 959–63.

Sellers, P. J. (1987). Canopy reflectance, photosynthesis, and transpiration. II. The role of biosphysics in the linearity of their interdependence. *Remote Sensing of Environment* **21**, 143–83.

Sellers, P. J., Berry, J. A., Collatz, G. J., Field, C. B., and Hall, F. G. (1992). Canopy reflectance, photosynthesis and transpiration. III. A reanalysis using improved leaf models and a new canopy integration scheme. *Remote Sensing of Environment* (in press).

Sellers, P. J., Mintz, Y., Sud, Y. C., and Dalcher, A. (1986). A simple biosphere model (SiB) for use within general circulation models. *Journal of Atmospheric Science* **43**, 505–31.

Shukla, J., Nobre, C., and Sellers, P. (1990). Amazon deforestation and climate change. *Science* **247**, 1322–5.

Stewart, J. B. (1988). Modelling surface conductance of pine forests. *Agricultural and Forest Meteorology* **43**, 19–35.

Tenhunen, J. D., Salal Serra, A., Harley, P. C., Dougherty, R. L., and Reynolds, J. F. (1990). Factors influencing carbon fixation and water use by mediterranean sclerophyll shrubs during summer drought. *Oecologia* **82**, 381–93.

Wong, S. C. (1979). Elevated atmospheric partial pressure of CO_2 and plant growth. I. Interactions of nitrogen nutrition and photosynthetic capacity in C_3 and C_4 plants. *Oecologia* **44**, 68–74.

Wong, S. C., Cowan, I. R., and Farquhar, G. D. (1979). Stomatal conductance correlates with photosynthetic capacity. *Nature* **282**, 424–6.

Wong, S. C., Cowan, I. R., and Farquhar, G. D. (1985*a*). Conductance in relation to rate of CO_2 assimilation. I. Influence of nitrogen nutrition, phosphorus nutrition, photon flux density and ambient partial pressure of CO_2 during ontogeny. *Plant Physiology* **78**, 821–5.

Wong, S. C., Cowan, I. R., and Farquhar, G. D. (1985*b*). Leaf conductance in relation to rate of CO_2 assimilation. III. Influences of water stress and photoinhibition. *Plant Physiology* **78**, 830–4.

Woodrow, I. E., and Berry, J. A. (1988). Enzymatic regulation of photosynthetic CO_2 fixation in C_3 plants. *Annual Review of Plant Physiology* **39**, 533–94.

Appendix A.

Intercellular Transport Model of C_4 Photosynthesis

Berry and Farquhar (1978) proposed the following expression to describe C_4 photosynthesis:

$$A = W_p - L\,, \tag{1A}$$

where W_p is the activity of PEP carboxylase and L is the leak of inorganic carbon between the bundle sheath cells and the intercellular spaces of the leaf mesophyll. A is assumed to be equal to the rate of net CO_2 fixation in the bundle sheath chloroplasts which is a function

of the CO_2 and O_2 partial pressures in the bundle sheath cells. Using the expression for rubisco-limited C_3 photosynthesis which takes into account photorespiration (Farquhar *et al.* 1980), A can also be expressed as

$$A = \frac{V_{max}\left(p_{bs} - \frac{0{\cdot}5O_{bs}}{\tau}\right)}{p_{bs} + K_c\left(1 + \frac{O_{bs}}{K_o}\right)}. \tag{2A}$$

Likewise the light-limited net CO_2 fixation in the bundle sheath is given as

$$A = a\alpha_r f Q_p \frac{p_{bs} - \frac{0{\cdot}5O_{bs}}{\tau}}{p_{bs} + \frac{1{\cdot}17O_{bs}}{\tau}}, \tag{3A}$$

where V_{max} is the capacity for CO_2 fixation by rubisco at saturating substrate concentrations, K_c is the Michaelis Constant for CO_2, K_o is the competitive inhibition constant, p_{bs} and O_{bs} are the bundle sheath CO_2 and O_2 partial pressures respectively, τ is the specificity of rubisco for CO_2 relative to O_2, α_r is the intrinsic quantum efficiency for CO_2 fixation (or the reciprocal of the quantum requirement for the production of RuBP), Q_p is the quantum flux density incident on the leaf and f is the fraction of absorbed Q_p that is used for production of RuBP. The constant 1·17 reflects the extra light-generated ATP required by photorespiration (see Berry and Farquhar 1978).

We used somewhat simpler expressions than Berry and Farquhar (1978) for the dependence of W_p on CO_2 and Q_p. CO_2-limited mesophyll photosynthesis is defined as

$$W_p = k_p p_i / P, \tag{4A}$$

where p_i is the CO_2 concentration in the intercellular spaces of the mesophyll. The apparent first order rate constant for CO_2, k_p, is in theory the ratio of V_{max}/K_m of PEP carboxylase at the pH of the mesophyll cells. Empirically it may be derived from the initial slope of CO_2 response curves of leaves (Fig. 2 and Table 1). Note that k derived in this manner would also include any non-stomatal resistance to CO_2 transport from the intercellular spaces to the sites of fixation.

The light-limited W_p is defined as

$$W_p = a\alpha_p(1 - f)Q_p, \tag{5A}$$

where α_p is the reciprocal of the quantum requirement for the production of PEP. The term $1 - f$ refers to the proportion of absorbed Q_p linked to the production of PEP.

The leak of CO_2 between the bundle sheath and the mesophyll is simply expressed by

$$L = (p_{bs} - p_i)/Pr_c, \tag{6A}$$

where r_c is the resistance to CO_2 diffusion through the bundle sheath cell walls and membranes. Large gradients in both HCO_3^- and CO_2 concentrations between the bundle sheath and the mesophyll may occur but the resistance to HCO_3^- diffusion is estimated to be ten times larger than to CO_2 diffusion (Furbank *et al.* 1989) so we neglect the former.

The rate of O_2 production and its diffusion between the bundle sheath and mesophyll is represented as

$$\lambda A = (O_{bs} - O_i)/PDr_c, \tag{7A}$$

where λ is the proportion of total net O_2 production occurring in the bundle sheath (corn bundle sheath chloroplasts show little photosystem II activity so λ is assumed to be small).

O_i is the partial pressure of O_2 in the intercellular spaces and D is a constant that takes into account the different solubilities and diffusivities of CO_2 and O_2 assuming that both gases diffuse along the same pathway.

Solving Eqns 6A and 7A for p_{bs} and O_{bs} respectively, and substituting these solutions into either the CO_2 limited (Eqns 2A and 4A) or the light limited (Eqns 3A and 5A) equations and combining with Eqn 1A yields a quadratic solution for either the CO_2 or light limited A_n in terms of the variables p_i, O_i, and Q_p;

$$aA^2 + bA + c = 0\,, \tag{8A}$$

where the coefficients are defined for the CO_2 and light limited conditions respectively as

$$a = \begin{cases} P\left(\dfrac{\lambda r_c D K_c}{K_o} - r_c\right) \\ P\left(\dfrac{\lambda D 1{\cdot}17}{\tau} - r_c\right) \end{cases};$$

$$b = \begin{cases} Pr_c p_i k_p + p_i + K_c + \dfrac{O_i K_c}{K_o} + \dfrac{0{\cdot}5\lambda Pr_c D V_{max}}{\tau} + V_{max} Pr_c \\ a\alpha_p(1-f)Pr_c Q_p + p_i + \dfrac{1{\cdot}17 O_i}{\tau} + \dfrac{0{\cdot}5a\alpha_r f Q_p \lambda Pr_c D}{\tau} + a\alpha_r f Q_p Pr_c \end{cases};$$

$$c = \begin{cases} V_{max}\left(\dfrac{0{\cdot}5O_i}{\tau} - Pr_c k_p p_i - p_i\right) \\ a\alpha_r f Q_p\left(\dfrac{0{\cdot}5O_i}{\tau} - a\alpha_p(1-f)Q_p Pr_c - p_i\right) \end{cases}.$$

The predicted response of the cellular model to CO_2 using parameters listed in Table 1 in comparison to those predicted by the leaf model and measured from a corn leaf at 25°C is shown in Fig. 2. The CO_2 limited region of the curve expresses the limitation imposed by PEP carboxylase activity while the CO_2 saturated region expresses the limitation by the rubisco capacity (V_{max}). The curvature in the transition between limitations is primarily a function of r_c, K_c, K_o and the ratio of k_p to V_{max}. Increasing r_c, K_o, k_p/V_{max} or decreasing K_c causes more abrupt saturation with respect to CO_2. Other parameters (O_i, λ, τ, D) have relatively small influence on curvature in the region of transition between CO_2 limited and CO_2 saturated rates. The cellular model overestimates A at high CO_2 levels because in this simulation A is assumed to be independent of the quantum flux while measured rates and those predicted by the simplified model are not completely light saturated.

Preliminary analysis of Eqn 8A has shown some interesting behaviours of the ICT model. First, there exists an optimum value for f which is dependent in particular on r_c and Q_p. The optimum value for f (the value which maximises A) is close to 0·6. The quantum requirement for RuBP re-generation in the absence of photorespiration relative to the total quantum requirement for PEP and RuBP re-generation is about 0·6. The optimum value of f increases as Q_p goes to zero.

Another interesting model response occurs at very low quantum fluxes. When A approaches zero it is obvious that p_{bs} will equal p_i (in the absence of dark respiration, R_d). As Q_p increases, p_{bs} increases, which causes the quantum yield to increase as photorespiration is inhibited. When Q_p is above about 50 μmol m^{-2} s^{-1} photorespiration is largely inhibited and the quantum yield becomes constant with increasing Q_p. The large changes in the degree to which rubisco is CO_2-limited over the range of quantum fluxes from 0–50 μmol m^{-2} s^{-1} implies that discrimination by rubisco against ^{13}C relative to ^{12}C will decrease with increasing light over this range.

Appendix B.

Equations Describing the Coupled Photosynthesis–Stomatal Conductance Model

The C_4 leaf model is derived from the following equations that define the three unknowns, stomatal conductance (g), net photosynthesis (A_n) and the partial pressure of CO_2 in the intercellular spaces of the leaf (p_i).

Following Ball *et al.* (1987) stomatal conductance is given by

$$g = m\frac{h_s A_n P}{p_s} + b\,, \tag{1B}$$

where h_s is the leaf surface relative humidity, P is atmospheric pressure, p_s is leaf surface partial pressure of CO_2 and m and b are the slope and intercept of a linear regression with respect to the other variables in the equation.

Gross photosynthesis (A) is given as a function of incident quantum flux density (Q_p) and the intercellular partial pressure of CO_2 (p_i) and leaf temperature (T_l) in the form of a pair of nested quadratic equations. The first quadratic is expressed as

$$\theta M^2 - M(V_T + \alpha Q_p) + V_T \alpha Q_p = 0\,, \tag{2B}$$

where V_T is the temperature-dependent, substrate-saturated rubisco capacity, α is the quantum efficiency and M is the flux determined by the rubisco and light limited capacities. The curavture parameter θ gives a gradual transition between the light limited and V_T limited flux. The limitation on the overall rate by M and the CO_2 limited flux, ($k_T p_i/P$), where k_T is the temperature-dependent pseudo-first order rate constant with respect to p_i, is likewise expressed as a quadratic

$$\beta A^2 - A(M + k_T p_i/P) + M k_T p_i/P = 0\,. \tag{3B}$$

β is analogous to θ and specifies the degree of co-limitation between M and the CO_2 limited flux. The smaller roots are the appropriate solutions for both quadratics. A_n is defined as

$$A_n = A - R_T\,, \tag{4B}$$

where R_T is the temperature-dependent rate of leaf respiration. The temperature dependence of the substrate saturated rubisco capacity (V_{max}), the pseudo-first order rate constant with respect to CO_2 (k) and the leaf respiration (R_T) are given as Q_{10} functions. V_{max} and R_d are also adjusted with inhibition functions that place upper and lower temperature limits on A_n. These limits were adjusted to approximate responses of C_4 plants to extreme temperatures (see Berry and Björkman 1980). The temperature dependencies are given as follows.

$$V_T = \frac{V_{max} Q_{10}^{\frac{T_l - 25}{10}}}{(1 + e^{0.3(13 - T_l)})(1 + e^{0.3(T_l - 36)})}\,;$$

$$R_T = \frac{R_d Q_{10}^{\frac{T_l - 25}{10}}}{1 + e^{1.3(T_l - 55)}}\,; \tag{5B}$$

$$k_T = k Q_{10}^{\frac{T_l - 25}{10}}\,,$$

where Q_{10} is the proportional increase in a parameter value for a 10°C increase in leaf temperature (Table 2).

Finally, the partial pressure of CO_2 in the intercellular spaces is defined as

$$p_i = p_s - \frac{1{\cdot}6A_n P}{g}. \tag{6B}$$

The solution to these simultaneous equations can be obtained by substitution to yield a cubic equation which is described further in Appendix C. Alternatively, a numerical solution may be used which could include consideration of diffusion through the leaf boundary layer and of the leaf energy balance, as was done for the C_3 model of Collatz *et al.* (1991).

Appendix C.

Analytical Solution to the Coupled Photosynthesis-Stomatal Conductance Model

Eqns 1B through 6B can be combined to eliminate p_i and g to yield a cubic equation,

$$a'A_n^3 + b'A_n^2 + c'A_n + d' = 0, \tag{1C}$$

where the coefficients are defined as

$$a' = \beta m h_s \frac{P}{p_s};$$

$$b' = \beta b - \beta m h_s R_T \frac{P}{p_s} + 1{\cdot}6k_T - Mmh_s \frac{P}{p_s} - k_T m h_s;$$

$$c' = R_T M m h_s \frac{P}{p_s} - Mb + R_T k_T m h_s - k_T b \frac{p_s}{P} - 1{\cdot}6k_T R_T + Mk_T m h_s - 1{\cdot}6k_T M;$$

$$d' = Mk_T b \frac{p_s}{P} + 1{\cdot}6Mk_T R_T - Mk_T m h_s R_T.$$

An explicit solution to Eqn 1C can be obtained and the same root was found to be applicable for widely different CO_2, light and temperature conditions. The solution is given by the following root

$$A_n = -2\sqrt{Q}\cos\left(\frac{S + 4\pi}{3}\right) - \frac{b'}{3a'}, \tag{2C}$$

where Q, S and R are defined as

$$Q = \frac{\left(\frac{b'}{a'}\right)^2 - 3\frac{c'}{a'}}{9};$$

$$R = \frac{2\left(\frac{b'}{a'}\right)^2 - 9\frac{b'c'}{a'^2} + 27\frac{d'}{a'}}{54};$$

$$S = \arccos\left(\frac{R}{\sqrt{Q^3}}\right)$$

(see Press *et al.* 1989).

The solution for A_n can be substituted into Eqn 1B of Appendix *B* to give g. Fig. 8*B* and *C* show the responses of g calculated in this manner to surface relative humidity.

Manuscript received 4 March 1992, accepted 19 May 1992